DNA Repair 129 (2023) 103541

Contents lists available at ScienceDirect

DNA Repair

journal homepage: www.elsevier.com/locate/dnarepair

Impairment of the non-catalytic subunit Dpb2 of DNA Pol ε results in increased involvement of Pol δ on the leading strand

Michal Dmowski [a,*], Karolina Makiela-Dzbenska [a], Sushma Sharma [b], Andrei Chabes [b], Iwona J. Fijalkowska [a,*]

[a] Institute of Biochemistry and Biophysics, Polish Academy of Sciences, Pawinskiego 5A, 02-106 Warsaw, Poland
[b] Department of Medical Biochemistry and Biophysics, Umeå University, SE-901 87 Umeå, Sweden

ARTICLE INFO

Keywords:
DNA polymerase epsilon
Pol ε
Dpb2
DNA polymerase delta
Pol δ
CMG (Cdc45 Mcm2–7 GINS)
Replication fork
DNA replication fidelity
Genome stability

ABSTRACT

The generally accepted model assumes that leading strand synthesis is performed by Pol ε, while lagging-strand synthesis is catalyzed by Pol δ. Pol ε has been shown to target the leading strand by interacting with the CMG helicase [Cdc45 Mcm2–7 GINS(Psf1–3, Sld5)]. Proper functioning of the CMG-Pol ε, the helicase-polymerase complex is essential for its progression and the fidelity of DNA replication. Dpb2p, the essential non-catalytic subunit of Pol ε plays a key role in maintaining the correct architecture of the replisome by acting as a link between Pol ε and the CMG complex. Using a temperature-sensitive *dpb2–100* mutant previously isolated in our laboratory, and a genetic system which takes advantage of a distinct mutational signature of the Pol δ-L612M variant which allows detection of the involvement of Pol δ in the replication of particular DNA strands we show that in yeast cells with an impaired Dpb2 subunit, the contribution of Pol δ to the replication of the leading strand is significantly increased.

1. Introduction

Faithful and timely DNA replication is a tightly regulated process, dependent on the coordinated actions of many proteins forming the replisome. In eukaryotic cells, three DNA polymerases belonging to the B family of polymerases, i.e., α, δ, and ε, are responsible for most of the synthesis of newly formed DNA strands; for review, see [1]. Pol α is a heterotetramer with primase and polymerase activity [2] that initiates DNA synthesis, to be taken over later by Pol ε or Pol δ replicating the leading and lagging strand, respectively, in advancing uninterrupted replication forks. However, recent discoveries have complicated this simple division of labor during DNA replication between the two polymerases as Pol δ has been shown to be involved in initiation, elongation, and termination of synthesis on the leading strand [1].

Pol δ is composed of the catalytic Pol3 subunit exhibiting polymerase and 3'→5' proofreading exonuclease activities and two non-catalytic Pol31 and Pol32 subunits [3,4]. Pol ε consists of 4 subunits, Pol2, Dpb2, Dpb3, and Dpb4 [5,6]. Pol2 is the catalytic subunit, and its N-terminal catalytic part (N-Pol2) equipped with DNA polymerase activity and a proofreading 3′→5′ exonuclease activity is responsible for DNA synthesis [7,8]. It is thought that the C-terminal part of Pol2 (C-Pol2) contains a second polymerase fold that has been inactivated during evolution [9]. Unlike the N-catalytic part of Pol ε, which has been shown to be dispensable, the non-catalytic C-Pol2 is essential for viability. [10,11]. Pol ε interacts with the replicative, 11-subunit CMG [Cdc45, Mcm2–7, and GINS (Psf1–3, Sld5)] helicase to form the CMGE complex [12–14]. The C-terminal part of Pol2 interacts directly with Dpb2 [15] and with Mcm2, Mcm5 subunits of the heterohexameric Mcm2–7 complex that builds the CMG helicase engine [12,15,16]. Dpb2 is the second largest subunit of Pol ε [17] and is conserved in eukaryotic polymerases [18,19]. Although Dpb2 has no catalytic activity, it is essential for viability. Dpb2 contains an N-terminal, helical domain, an oligonucleotide/oligosaccharide-binding (OB) domain, and an inactivated calcineurin-like phosphoesterase (PDE) domain [20,21]. Interestingly, according to a recently proposed model, the OB fold in Dbp2 directs leading ssDNA from CMG to the Pol ε active site [22]. Within the replisome, Dpb2 interacts with the GINS subunit Psf1, the helicase core subunit Mcm3 and Cdc45 [13,15,22–24]. Previously we found that Dpb2 is important for the faithful replication of genomic DNA and activation of the replication checkpoint [25–27]. Dpb2p plays a key role in maintaining the correct architecture of the replisome by acting as a link between Pol ε and the CMG complex [12,13,28]. Pol ε and CMG

* Corresponding authors.
E-mail addresses: mdmowski@ibb.waw.pl (M. Dmowski), iwonaf@ibb.waw.pl (I.J. Fijalkowska).

https://doi.org/10.1016/j.dnarep.2023.103541
Received 31 March 2023; Received in revised form 29 May 2023; Accepted 5 July 2023
Available online 7 July 2023

interact functionally. Pol ε modulates the activity of the CMG helicase while CMG has a stimulating effect on Pol ε [29–31] and directs Pol ε to the leading strand [12,13]. Dpb3 and Dpb4 subunits of Pol ε are not essential, ancillary, DNA-binding subunits that adopt histone folds [32,33]. Importantly Dpb3-Dpb4 bridge the catalytic and non-catalytic modules of Pol2 [22], and are required for epigenetic inheritance during DNA replication [34,35].

Biochemical and structural studies provided important data on the major enzymatic activities and the overall architecture of the eukaryotic replisome and revealed the basic principles of genomic DNA duplication. However, the physiological role of specific subunits of the replisome, in particular the non-catalytic subunits, is still poorly understood. There is also a lack of data on the physiological consequences of defects in the function of individual proteins. With an increasing number of reports linking physiological defects leading to severe disease to mutations in non-catalytic proteins of the replisome [36–38], this knowledge is fundamental.

Previously, we have isolated a number of temperature-sensitive *dpb2* mutants encoding Dpb2 variants demonstrating defective interaction with the C-domain of the Pol2 catalytic subunit and the Psf1 subunit of the GINS helicase [25,39]. Strains carrying these mutations show phenotypes indicative of impaired DNA replication and a strong mutator effect comparable in size to a defective mismatch repair (MMR) mechanism (*msh6*Δ) or the lack of Pol ε's 3'→5' exonuclease activity (*pol2–4*) [25,39]. Here, we employed the *dpb2–100* allele encoding a Dpb2 variant with L284P and T345A substitutions [25]. Previously we showed that Pol ε complex isolated from the *dpb2–100* strain contains substoichiometric amounts of the Dpb2 subunit [39]. In the *dpb2–100* strain, the contribution of error-prone Pol ζ to DNA synthesis is increased [39,40]. Dpb2 defect causing reduced interaction with the C-terminal part of Pol2 and, at the same time, with the Psf1 subunit of the GINS complex, can weaken the cooperation of CMG with Pol ε and reduce the stability of Pol ε during replication of the leading strand. This, in turn, may result in an increased contribution of Pol δ to the replication of this strand. To verify this hypothesis, we used a well-described yeast genetic system that Kunkel's laboratory used to identify the activity of Pol δ and Pol ε on the two replicated DNA strands [41–43]. This system takes advantage of a distinct mutational signature of the Pol δ-L612M variant and allows detection of the involvement of Pol δ in the replication of particular DNA strands in yeast cells [42]. We show that in cells with an impaired Dpb2 subunit, the contribution of Pol δ to the replication of the leading strand is significantly increased.

2. Results

2.1. The experimental approach to study the involvement of Pol δ in leading/lagging strand replication

To investigate the possible contribution of DNA polymerase δ in the replication of the leading strand in the *dpb2–100* mutant, we used a genetic system that we recently employed to study the involvement of Pol δ in yeast cells with impaired CMG helicase function [44]. The Pol δ-L612M variant used in this approach introduces specific mutations during DNA replication, which allows tracking of Pol δ on particular DNA strands [45]. The spectrum of mutagenesis is analyzed in cells with the *URA3* reporter gene cloned in two orientations regarding the nearest origin of replication ARS306 (~2 kb distance, compared to ~32 kb from ARS307) [42]. As a consequence, the *URA3* coding sequence in one strain serves as a template for lagging strand (orientation 1 [OR1]) or for leading strand in the other strain (orientation 2 [OR2]) (Fig. 1). Therefore, in *URA3*[OR1] T•dGTP, C•dTTP, and G•dTTP mispairs, most commonly introduced by Pol δ-L612M, result in T→C, C→A, and G→A substitutions in the reporter gene coding sequence, respectively [46,47]. Similarly, in *URA3*[OR2], the same mispairs result in A→G, G→T, and

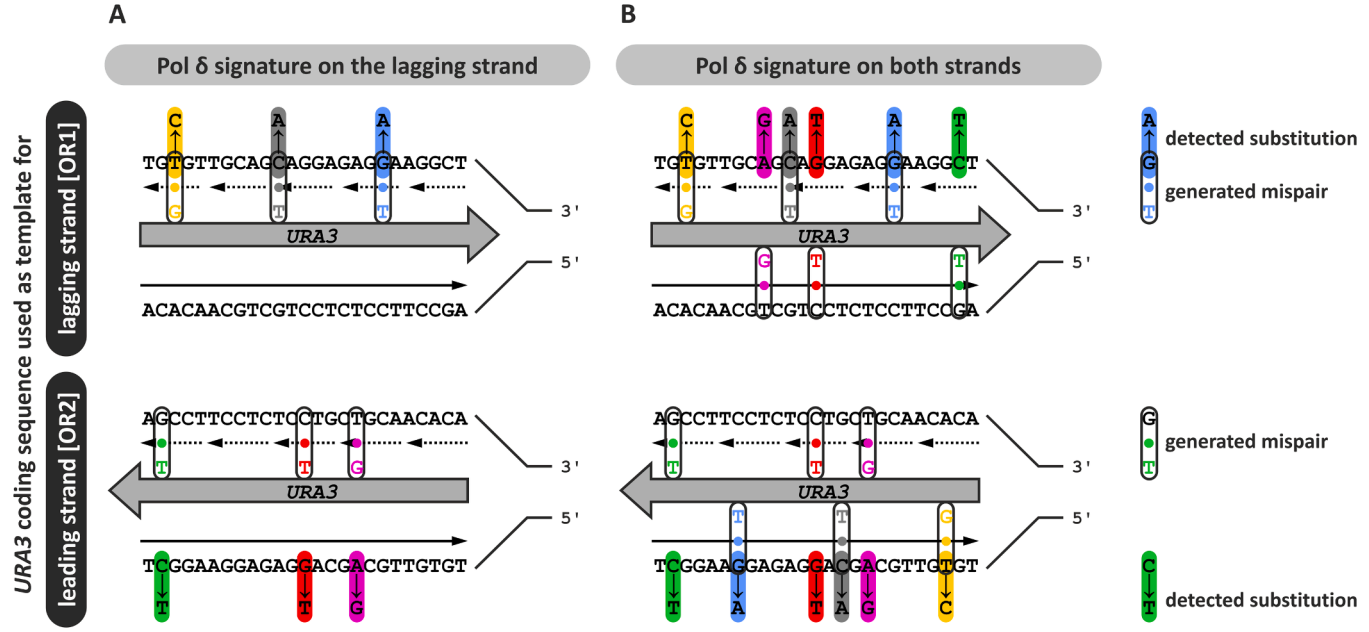

Fig. 1. The rationale for the analysis of the Pol δ contribution to leading strand replication in the *dpb2–100* mutant. **(A)** The *URA3* reporter gene was cloned in one orientation in strains [OR1] and in opposite orientation in strains [OR2] in the vicinity of ARS306. Therefore, its coding sequence was lagging-strand template in OR1 and a leading-strand template in OR2. As a result, L612M Pol δ–specific T•dGTP, C•dTTP, and G•dTTP mispairs generated during lagging strand replication were detected in *URA3* OR1 as T→C, C→A, and G→A substitutions, respectively. In the *URA3* OR2, the same mispairs were detected as A→G, G→T, and C→T substitutions. **(B)** If Pol δ additionally contributed to the replication of the leading strand, L612M Pol δ – specific mispairs would be generated in both strands. In this case, in *URA3* OR1, a G•dTTP mispair generated during lagging strand replication would be detected as a G→A substitution, while the mispair generated during leading strand replication would be detected as a C→T substitution. Accordingly, in *URA3* OR2, a G•dTTP mispair generated during lagging strand replication would be detected as a C→T substitution, while when generated during leading strand replication, it would be detected as a G→A substitution.

C→T substitutions, respectively. An analysis of mutation spectra in *URA3* in cells carrying the *pol3-L612M* and *dpb2–100* alleles and a comparison with results obtained in *pol3-L612M DPB2* cells enabled the estimation of the contribution of Pol δ in leading strand replication. Because earlier studies have shown that increased mutation rates in *dpb2–100* cells are partially dependent on the error-prone Pol ζ [40], and that the introduced errors are corrected by the mismatch repair (MMR) mechanism [25], we performed an analysis of mutational spectra in the *rev3*Δ *msh6*Δ background. As a control, we used mutational spectra data obtained for strains described as *DPB2 POL3* OR1, *DPB2 POL3* OR2, *DPB2 pol3-L612M* OR1, and *DPB2 pol3-L612M* OR2 (all in the *rev3*Δ *msh6*Δ background), and presented in our previously published work [44].

First, we compared the contribution of each type of substitution to the total mutational spectrum (Fig. 2). In *pol3-L612M* cells with *URA3*-OR1 T→C and G→A changes accounted for 30% and 61% of all mutations, respectively, and in *pol3-L612M* cells with *URA3*-OR2 the most abundant substitutions are C→T and G→T - 49% and 27%, respectively. In *dpb2–100* derivatives of these strains, we observed significant changes: in *pol3-L612M dpb2–100* [OR1] strains in comparision with *pol3-L612M* [OR1] the share of T→C and G→A substitutions in the spectrum of mutations significantly declined (19% and 54% of all mutations, respectively) and the fraction of C→T and G→T substitutions increased (from ~1% to 12% and from ~1% to 6%, respectively) ($p = 0.0030$). In *pol3-L612M dpb2–100* [OR2] compared to *pol3-L612M* [OR2] cells the share of C→T and G→T substitutions decreased to 42% and 17%, respectively. Likewise, the contribution of T→C and G→A substitutions increased from 1% and 5%, to 5% and 17%, respectively ($p = 0.0086$). A more detailed analysis of changes in mutation spectra in cells with the *dpb2–100* allele is shown below.

2.2. AT→GC, CG→TA, and GC→TA substitutions in dpb2-100 cells

As we have previously shown [44], in the genetic background used in this work, in *pol3-L612M URA3*[OR1] cells, A-T→G-C substitutions originating from T→C changes in the *URA3* coding sequence were observed > 53x more frequently than A→G, while in *pol3-L612M URA3* [OR2] the same ratio was 0.1 (Fig. 3A) [44]. Similarly, in these strains, the ratio of C-G→T-A transitions originating from G→A versus C→T changes was 107 in *URA3*[OR1] and 0.1 *URA3*[OR2] (Fig. 3A). Another type of substitutions that demonstrated different ratios of nucleotide changes depending on the orientation of the reporter gene *URA3* are G-C→T-A substitutions [44,46]. In *pol3-L612M* cells, the C→A versus G→T ratio was 2 and < 0.02 in *URA3*[OR1] and *URA3*[OR2], respectively (Fig. 3A). The strong *URA3* orientation bias observed for these substitutions is consistent with the specificity of mismatches produced by Polδ-L612M and the involvement of this polymerase mainly in lagging strand replication [45].

The presence of the *dpb2–100* allele in *pol3-L612M* cells significantly changed the ratios observed. The T→C versus A→G ratio in *URA3*[OR1] was reduced to > 27 ($p < 0.0001$), while in *URA3*[OR2] it increased to 0.5 ($p < 0.0001$) (Fig. 3B and Table S1 and S2). Similarly, the rate of G→A relative to C→T was reduced to 4.4 in *pol3-L612M dpb2–100 URA3* [OR1] ($p < 0.0001$), and increased to 0.4 in *pol3-L612M dpb2–100 URA3*[OR2] ($p < 0.0001$) (Fig. 3B and Table S1 and S2). Importantly, the Tarone test used to compare the ratios of G→A versus C→T substitutions in the two orientations of the reporter gene gave the *p*-value < 0.0001. The *dpb2–100* allele also affected the ratio of C→A versus G→T substitutions; it was reduced to 0.5 ($p < 0.0001$) (Table S2) when the reporter gene was in [OR1], and increased to 0.01 ($p < 0.0001$) in *URA3*[OR2] (Fig. 3B and Table S1 and S2). Again, the Tarone test used to compare the ratios of C→A versus G→T substitutions in the two orientations of the reporter gene gave a *p*-value < 0.0001.

We conclude that the observed changes in mutagenesis spectra in cells with the *dpb2–100* allele result from T•dGTP, G•dTTP, and C•dTTP mispairs generated by Pol δ-L612M during replication of the leading strand.

2.3. Mutations generated by Pol δ-L612M at specific hotspots in dpb2-100 cells

As was shown previously, Pol δ-L612M-specific mutations were generated at increased rates at specific hotspots in the *URA3* reporter gene [42,44,48]. In *URA3*[OR1], these are at position 97 for T→C substitutions and 764 for G→A, while in *URA3*[OR2], specific hotspots were observed at position 310 for C→T and 679/706 for G→T (Fig. 4A). Here we show that rates at specific hotspots are significantly changed in *dpb2–100* cells. The rate of T→C substitutions at position 97 was > 26-fold higher in *URA3* OR1 than in *URA3* OR2 in *pol3-L612M* cells, but only 2.5-fold higher in *pol3-L612M dpb2–100* cells (Fig. 4) ($p < 0.0001$, Table S3). The rate of this type of substitution at other sites was 16-fold higher in *URA3* OR1 than in *URA3* OR2 in *pol3-L612M* cells and was reduced to 3 in cells with the *dpb2–100* allele (Fig. 4) ($p < 0.0001$, Table S4). Similarly, in *pol3-L612M* the rate of G→A changes was higher in *URA3* OR1 than in *URA3* OR2 24-fold at position 764 and 13-fold at other positions (Fig. 4) ($p < 0.0001$, Table S3). In the presence of the *dpb2–100* allele, these values were reduced to 3.2 and 2.0, respectively(Fig. 4)($p < 0.0001$, Table S4). The rate of C→T substitutions in *pol3-L612M* cells is more than 39-fold higher in *URA3* OR2 than in *URA3* OR1 both at the hotspot at position 310 and at other sites (Fig. 4)($p < 0.0001$, Table S3 and S4). In *pol3-L612M dpb2–100* cells, this dominance was reduced to 13-fold and 2-fold at the hotspot at position 310 and at other sites, respectively (Fig. 4) ($p < 0.0001$, Table S3 and S4). Finally, the G→T substitutions which in *pol3-L612M URA3* OR2 compared to *pol3-L612M URA3* OR1 occurred at a rate > 8-fold higher at positions 679 and 706 and more than 18-fold higher at the other sites, in *pol3-L612M dpb2–100* OR2 cells occurred at the rates only 2.6 and 5.4-fold higher than in than in *pol3-L612M dpb2–100* OR1, respectively (Fig. 4)($p < 0.0001$, Table S3 and S4). In summary, these results show that mutation types that occurred with high prevalence in the

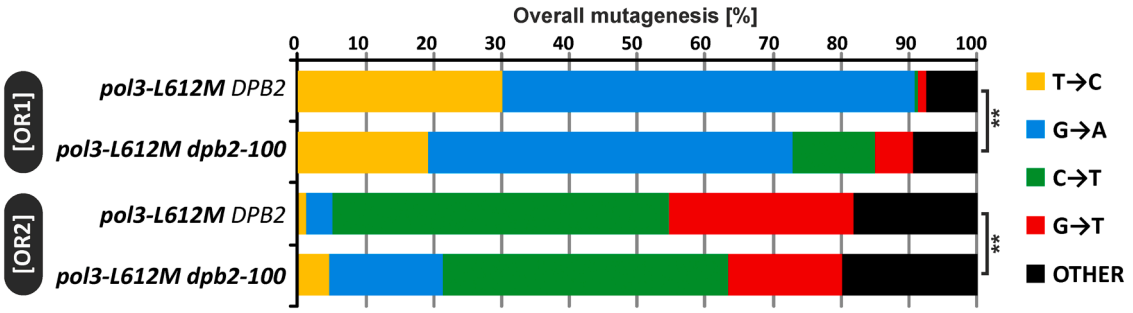

Fig. 2. Contribution of Pol δ-L612M-specific types of substitutions to total mutagenesis in strains with *pol3-L612M* or *pol3-L612M dpb2–100* alleles in the *rev3*Δ *msh6*Δ background. The reporter gene *URA3* was cloned in two orientations [OR1] and [OR2]. Mutation spectra were analyzed in the coding sequence of *URA3* from 5-FOA-resistant yeast clones. The proportion of each substitution type found in each spectrum is shown. Detailed data are provided in Table S1.

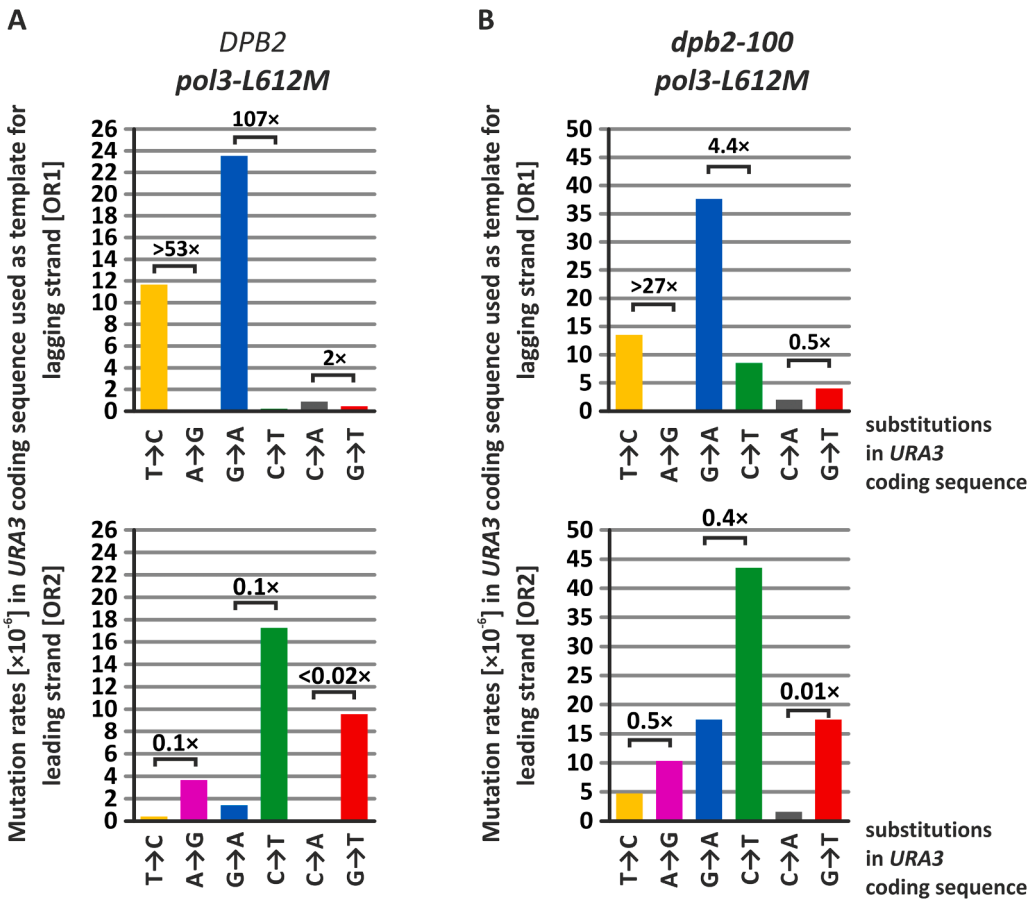

Fig. 3. Total mutation rates calculated for specific substitutions resulting in A-T→G-C, C-G→T-A, and C-G→A-T substitutions found in the *URA3* sequence [5-FOA^R× 10^{-6}] in strains with *pol3-L612M* **(A)** or *pol3-L612M dpb2–100* alleles **(B)** in the *rev3Δ msh6Δ* background. For detailed mutation spectra, see Table S1. The analysis of the statistical significance of the observed differences is shown in Table S2.

orientation in which the *URA3* coding sequence served as a lagging-strand template (T→C, and G→A changes in the *URA3* coding sequence) in cells with the *dpb2–100* allele were found at significantly increased rates in the reporter gene when the coding sequence served as the leading strand template. Similarly, substitutions specific to the other *URA3* orientation, where the coding sequence was the leading strand template (C→T and G→T changes in the *URA3* coding sequence), were introduced at significantly higher rates in *dpb2–100* cells where the *URA3* coding sequence served as the lagging strand template (compare Fig. 4A and B). In parallel, relative rates of substitutions specific for a given orientation in *pol3-L612M* cells decrease in *pol3-L612M dpb2–100* cells (Fig. 4A and B). These observations support the hypothesis that in *dpb2–100* cells, participation of Pol δ in leading strand replication is increased.

2.4. Cell cycle progression of dpb2-100 cells and the measurement of dNTP pools

Perturbations of DNA replication can delay progression through the S phase of the cell cycle. Therefore, we synchronized *dpb2–100* cells in the G1 phase using the α-factor and monitored their entry into a new cell cycle as changes in DNA content using the fluorescence-activated cell sorting method (FACS). Compared to wild-type cells, *dpb2–100* cells demonstrate a changed FACS profile with an increased population of cells in the S phase of the cell cycle (Fig. 5A). After release from the G1 block, *dpb2–100* cells progressed slowly through the S-phase and required more time to complete DNA synthesis. Cellular response to impaired DNA replication may involve an increase in the dNTP pool levels. Moreover, imbalanced concentrations of nucleotides accessible for DNA synthesis may have consequences for the specificity of mutations. To test this hypothesis, we analyzed the dNTP pool levels in *dpb2–100* cells. We observed an over 4-fold increase in the amounts of all nucleotides (Fig. 5B). However, the amounts of each nucleotide relative to each other were the same in *dpb2–100* cells as in wild-type cells therefore, should not have consequences for the specificity of mutations (Fig. 5C).

2.5. Analysis of the involvement of Pol ε in leading/lagging strand replication

Pol ε forms the pre-loading complex (pre-LC) loaded onto Mcm2–7 during DNA replication initiation. Importantly, depletion of Dpb2 in *S. cerevisiae* cells after synchronization in the G1 phase prevented the association of other pre-LC factors with Mcm2–7 [49]. In light of these observations, we considered the possibility that as a result of impaired interaction with Pol2 and Psf1, Dpb2–100 might compromise the assembly of replisomes resulting in inefficient firing of some origins. This would necessitate DNA replication initiation from a neighboring origin resulting, in inverted leading/lagging strand specificity, i.e., the DNA strand, which under normal conditions is replicated as the leading strand would be replicated as the lagging strand (by Pol δ), while the other one as the leading strand (by Pol ε). Therefore, we decided to test the hypothesis that the observed increased signature of Pol δ on the leading strand is the effect of *URA3* sequence replication performed by the replisome approaching from another neighboring origin. To do this, we analyzed the signature of Pol ε-M644G variant of the leading strand replicase. Replication by Pol ε-M644G is characterised by a high incidence of A-T→T-A transversions, occurring predominantly via the

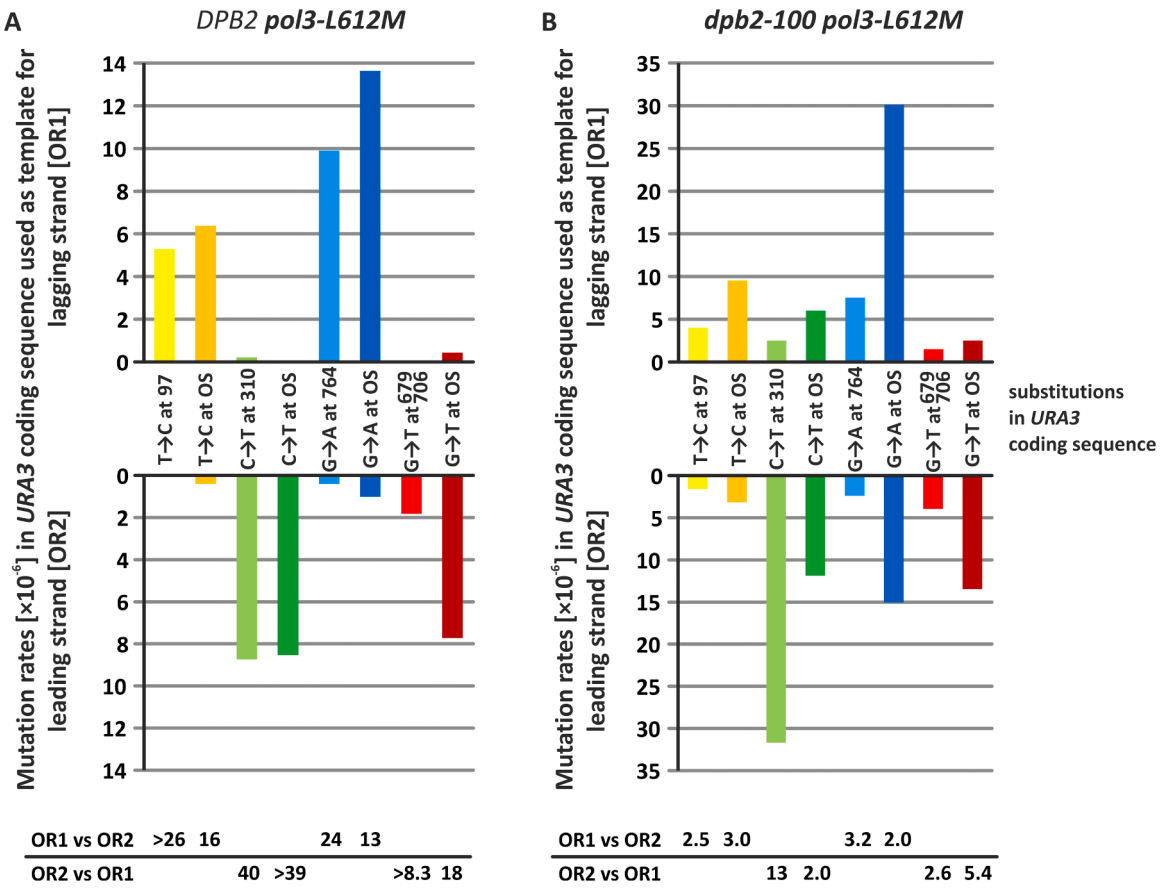

Fig. 4. Mutation rates calculated for specific substitutions in the *URA3* reporter gene at hotspots characteristic for the Pol3-L612M variant of Pol δ (positions 97, 310, 764, and 679/706) and other sites (OS) [5-FOA^R× 10^{-6}] in strains with *pol3-L612M* **(A)** or *pol3-L612M* and *dpb2–100* mutations **(B)** in the *rev3Δ msh6Δ* background. For detailed mutation spectra, see Table S1. In the *pol3-L612M* OR1 strain, the number of sites other than hotspots was 12 for T→C substitutions and 17 for G→A. In the *pol3-L612M* OR2 strain, the number of sites other than hotspots was 2 for T→C substitutions, 10 for C→T, 5 for G→A, and 15 for G→T. In the *pol3-L612M dpb2–100* OR1 strain, the number of sites other than hotspots was 12 for T→C substitutions, 8 for C→T, 18 for G→A, and 4 for G→T. In the *pol3-L612M dpb2–100* OR2 strain, the number of sites other than hotspots was 4 for T→C substitutions, 9 for C→T, 13 for G→A, and 10 for G→T. The analysis of the statistical significance of the observed differences is shown in Table S3 and Table S4.

T•dTTP mispairs rather than A•dATP transversions [43,50]. Consequently, the A-T→T-A transversions produced by Pol ε-M644G (in the *DPB2* strain) are manifested in the high rate of the A→T changes in the *URA3*[OR1] coding sequence and in the high rate of the T→A changes in *URA3*[OR2] (Fig. 6A and C). Conversly, if the reporter gene sequence was replicated by the replisome originating from another, more distant origin, the coding sequence would be the leading strand template in *URA3*[OR1] and as the lagging strand template in *URA3*[OR2] (Fig. 6B). As a result, in *pol2-M644G dpb2–100* cells one would expect an increased prevalence of T→A substitutions in *URA3*[OR1] and A→T in *URA3* [OR2], compared to the *pol2-M644G DPB2* strain (Fig. 6B). However, in *pol2-M644G dpb2–100* cells with *URA3*[OR1], the ratio of A→T rate versus T→A substitutions demonstrated no significant changes from 8.3 to 7.0 ($p = 0.2691$) (Fig. 6D upper part and Table S1 and S5). Consistently, when the reporter gene was in inversed orientation *URA3*[OR2], A→T mutations were observed neither in *pol2-M644G*, nor in *pol2-M644G dpb2–100* cells; and the ratio of A→T rate versus T→A substitutions was unchanged ($p > 0.9999$) (Fig. 6D lower part and Tables S1 and S5). Moreover, the Tarone test used to compare the ratios of A→T versus T→A substitutions in the two orientations of the reporter gene gave a *p*-value 0.9886. These results show that the involvement of Pol ε in DNA replication on both strands is not significantly changed in cells with the *dpb2–100* allele, compared to *DPB2* cells. Therefore, we conclude that the observed mutational signature of Pol δ on the leading strand in *dpb2–100* cells is not caused by an inversion of replication fork movement direction.

3. Discussion

At the eukaryotic replication fork, the highly conserved components of the replisome work together to facilitate replisome progression and maintain genome stability. Our current understanding of the division of labor among the major replicases predominantly results from research conducted on yeast. The generally accepted model assumes that leading strand synthesis is performed by Pol ε, while lagging-strand synthesis is catalyzed by Pol δ. Many experiments have confirmed this division of labor between polymerases. First of all, the employment of mutator variants of yeast polymerases producing specific mismatches (Y869A or L868M Pol α, L612M Pol δ, and M644G Pol ε), and analysis of the specificity of errors introduced into the reporter gene into both DNA strands allowed to determine the contribution of Pol ε and Pol δ to the synthesis of a particular DNA strand [41–43,51,52,53]. Additionally, the usage of different polymerases during replication has been mapped by Pol ε or Pol δ variants promiscuous for ribonucleotide incorporation [47, 52–59]. Additionally, the results of experiments in which replication was reconstituted in vitro using purified components support such division of labor between polymerases [12,60–63]. Finally, replisome architecture analysis also supports this canonical model during uninterrupted elongation [15,16,64].

Pol ε has been shown to target the leading strand by interacting with the CMG helicase [Cdc45-Mcm2–7-GINS(Psf1–3, Sld5)] [12,13,65,66]. This requires the interaction of the non-catalytic Dpb2 subunit of Pol ε with the Psf1 subunit of GINS, as well as with Mcm3 [13,15,23,24]. In

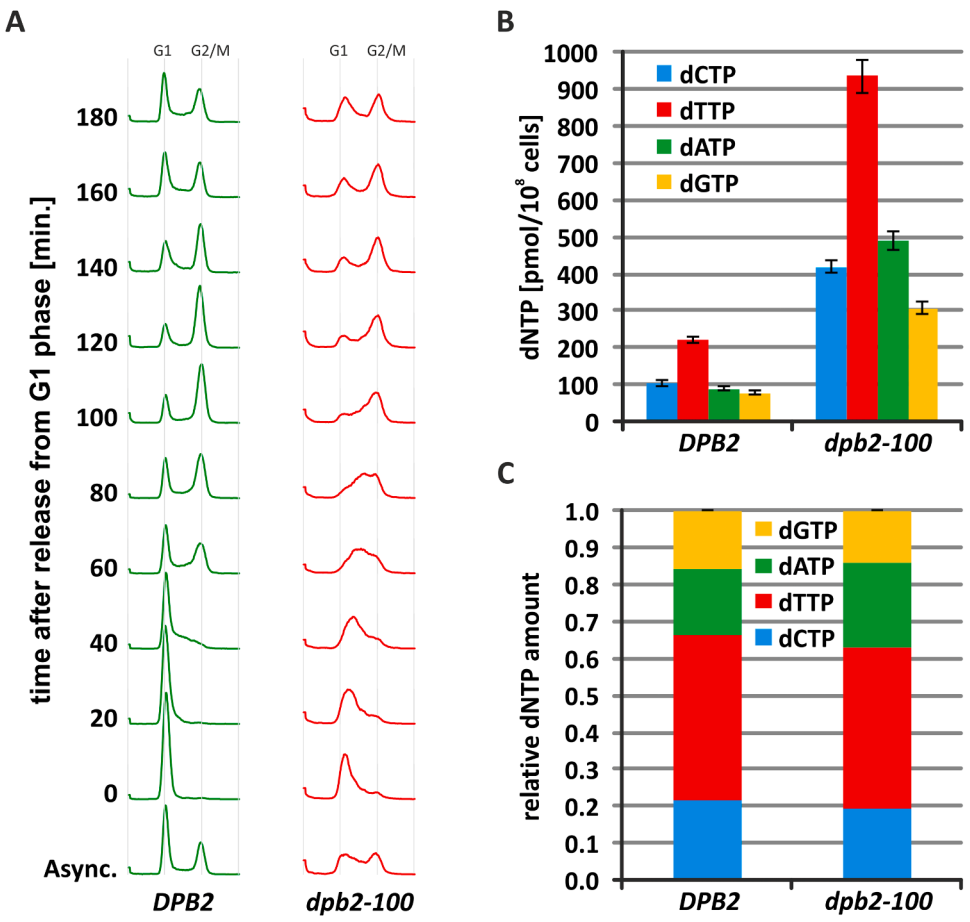

Fig. 5. Progression through the cell cycle and dNTP pool measurement in the *dpb2–100* mutant. **(A)** Flow cytometry (FACS) analysis of asynchronous cells and those released from the G1 block at the permissive temperature of 23 °C. Wild-type and *dpb2–100* mutant populations were analyzed. DNA content for G1 and G2/M are indicated. **(B)** Concentrations of the four dNTPs in *DPB2* and *dpb2–100* cells. Mean values with SD are shown. **(C)** Relative dNTP amounts in *DPB2* and *dpb2–100* cells calculated using data from B. For the analysis of statistical significance of the differences in the dNTP balance between *DPB2* and the *dpb2–100* strain, the contingency tables were compared using the chi-square test ($p = 0.1357$).

parallel, Pol δ access to the lagging strand is promoted by binding to PCNA [67], and the presence of RPA-coated ssDNA facilitates this targeting [62,63].

Recent genetic and biochemical data and high-resolution mapping of polymerase usage have identified new key roles for Pol δ in several steps of leading-strand synthesis; reviewed in [1]. First, Pol δ was shown to initiate the leading strand synthesis from the lagging strand primer from the opposite side of the origin [53,68–71]. Furthermore, Pol δ was found to synthesize both DNA strands during replication termination [57]. Additionally, during break-induced replication (BIR) [69] or when replication fork progression is blocked, Pol δ participates in homologous recombination (HR)-mediated restart of collapsed replication forks [72]. Furthermore, Pol δ can take over the replication of the leading strand when Pol ε is deprived of catalytic activity [71]. This defect (*pol2–16* mutation) results in severe growth defect, increased doubling time, larger than normal cells, mutator phenotype, aberrant nuclei, and higher than normal dNTP concentrations [46,71]. It has been shown that when the level of Pol ε in the cell is reduced, Pol δ is more likely to participate in DNA synthesis [46,57,71]. Furthermore, the presence of Pol δ on the leading strand is evidenced by the fact that Pol δ corrects Pol ε errors [73,74]. All these observations indicate that Pol δ is able to replace the replicative function of Pol ε.

Proper functioning of the CMGE complex is essential for the leading strand replisome, fidelity of DNA replication, and the rate of CMGE progression [23,62]. As mentioned earlier, the N-terminal part of the Pol2 catalytic subunit exhibits DNA polymerase and exonuclease activities [8], while the C-terminal part (C-Pol2) is predicted to contain a second polymerase fold but become inactivated during evolution [9,20]. C-Pol2 and the Dpb2 non-catalytic subunit are essential subunits required for CMGE formation and DNA replication. It was suggested that the OB fold in Dbp2 directs leading ssDNA from CMG to the Pol ε active site [22]. Additionally, the Dpb2 subunit stimulates CMG activity [12]. Dpb2 has been shown to share an extended interface with the C terminal half of Pol ε, indicating an important structural and stabilizing role for Dpb2 [15]. Remarkably, Dpb2 contacts Mcm3, while the C-Pol2 polymerase part contacts Mcm2 and Mcm5. These interactions allow for the closure of the Mcm2–5 gate on the ATPase side of the helicase motor ring [15]. Furthermore, the N-terminal part of Dpb2 links Pol ε to the GINS component of the CMG through Dpb2 - Psf1 interaction [15,23,24]. Thus, C-Pol2 and Dpb2 provide a molecular bridge linking CMG to Pol ε, with Dpb2 contacting GINS and C-Pol2 contacting MCM [15,24]. It can be assumed that a defect in the CMG - Pol ε interactions can not only cause disturbances of helicase function but also affect the stabilization and function of Pol ε during leading strand synthesis.

We employed the temperature-sensitive *dpb2–100* mutant previously isolated in our laboratory, to investigate what are the physiological consequences associated with the impairment of the Dpb2 subunit. We have previously shown that *dpb2–100* expression has a strong mutator effect and various phenotypes characteristic of replication mutants, i.e., dumbbell cells, and enlarged nuclei and cells. Here we also show that the *dpb2–100* strain has an increased nucleotide pool and strongly delayed cell cycle progression. We know from previous studies that the stoichiometry of the Pol ε subunits in the Pol $\varepsilon_{Dpb2–100}$ variant is significantly altered [39]. The Dpb2–100 (L284P, T345A) subunit is present at approximately 1/10 of its normal level (the Pol2:Dpb2–100:Dpb3:Dpb4 ratio is 1:0.1:1:1.2 instead of 1:1:1:1 [75]. In addition, the Dpb2–100 subunit has impaired interactions with the C-terminal part of Pol2 and with the Psf1 subunit of the GINS complex [39]. These data suggest that in vivo, there may be a reduced amount of CMGE complexes with the correct subunit composition. However, we have shown that Dpb2–100 does not alter the biochemical properties of Pol ε, including catalytic efficiency, processivity, or proofreading activity [39]. Interestingly, the

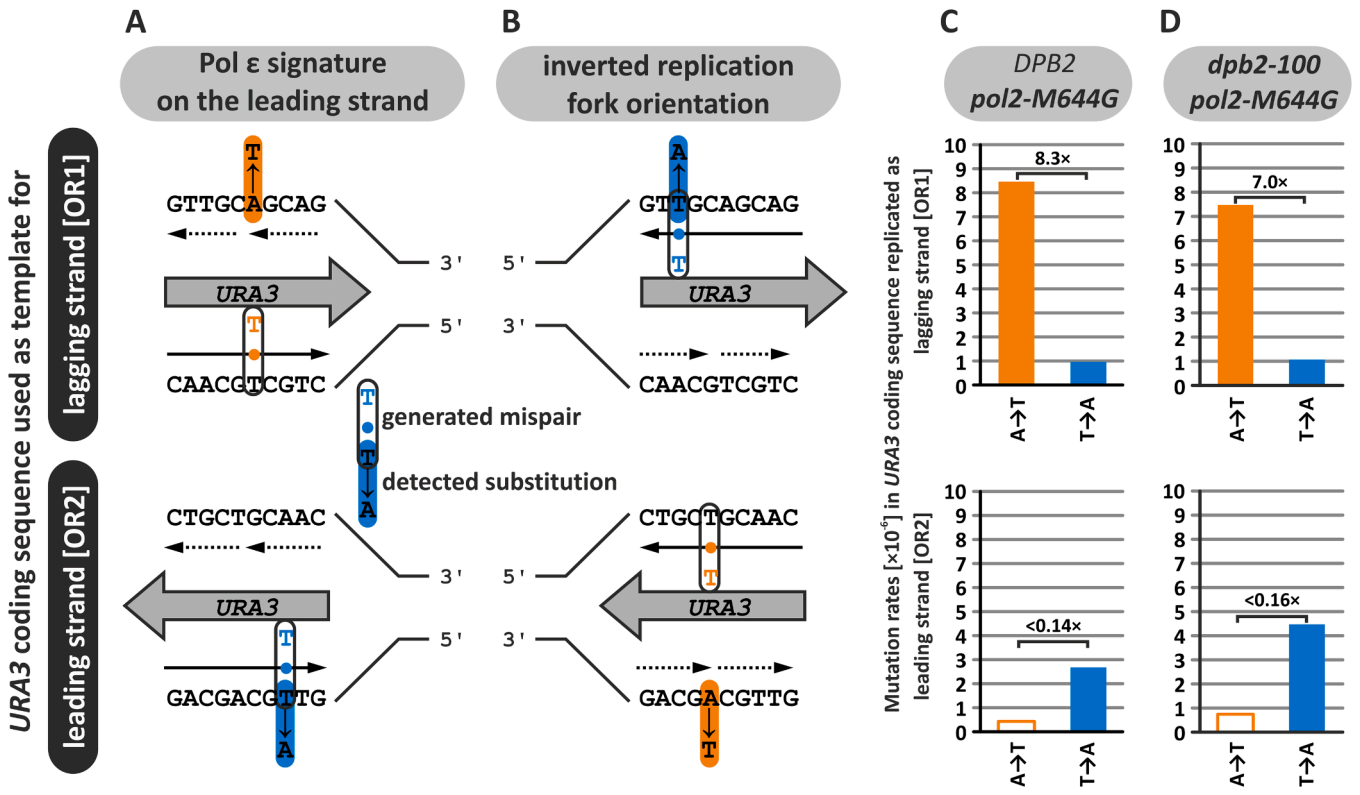

Fig. 6. Mutation rates calculated for specific substitutions [5-FOA^R× 10^{-6}] in strains with *pol2-M644G* or *pol2-M644G dpb2–100* alleles in the *rev3Δ msh6Δ* background. An open bar indicates the mutation rate that would be observed if a single event was detected. For detailed mutation spectra, see Table S1. The analysis of statistical significance of the observed differences is shown in Table S5.
Sections A and B of this figure originate from https://doi.org/10.1016/j.dib.2022.108223, an open-access article under the CCBY license http://creativecommons.org/licenses/by/4.0/.

synergistic effect of the *dpb2–100* and *pol3-L612M* mutations presented herein (Table S1) and the similar effect of *dpb2–100* and *pol3–5DV* (Pol δ with inactive proofreading) on mutagenesis rates observed previously [39] suggest that in the *dpb2–100* strain, the Pol δ holoenzyme may participate more efficiently in leading strand replication.

To investigate this, we used a genetic system developed in Kunkel's lab that allows analyzing mutations that arise on respective DNA strands as a result of errors made by a specified DNA polymerase. The reporter gene (here *URA3*) is cloned in two orientations regarding the nearest origin of replication. Therefore, in one strain [OR1] its coding sequence is replicated as the lagging but in the other [OR2] as the leading strand, thus elongated by Pol ε or Pol δ, respectively. The Pol δ-L612M variant introduces specific mispairs which, depending on the orientation ([OR1] or [OR2]) of the reporter, generate different substitutions in the coding sequence (Fig. 1). The results presented in this work demonstrate that substitutions identified as dominating in the *URA3* sequence in a given orientation in *pol3-L612M* cells, in *pol3-L612M dpb2–100* cells were found in the reporter gene when its sequence was in inversed orientation (Figs. 2, 3, and 4). Moreover, the analysis of the amount of the four nucleotides in *dpb2–100* cells has shown that although the dNTP pool was increased, presumably as a result of the intra S-phase checkpoint activation, the dNTP pool balance was maintained (Fig. 5). Therefore, we exclude the possibility that the relative changes in specific mispair rates are caused by an imbalanced dNTP pool. Finally, we checked whether the increased contribution of Pol δ to leading strand replication is caused by the simple inversion of the direction of movement of the replisome, which would come from a more distant ARS instead of the nearest ARS306. For this purpose, we analyzed the signature of the Pol ε-M644G variant to check whether this polymerase replicates the DNA strand, that under normal conditions is replicated as the lagging strand by Pol δ. We found no difference in relative A→T versus T→A rates between cells with *DPB2* and *dpb2–100* alleles (Fig. 6), demonstrating that the increased contribution of Pol δ to DNA synthesis on the leading strand is not caused by DNA replication starting from a neighboring origin.

Interestingly, using the same approach we have previously examined whether the *psf1–1* mutation in the GINS subunit of the CMG complex changes the canonical participation of DNA polymerases in the replication of leading and lagging DNA strands [44,50]. The obtained results have shown that the defect of the GINS complex causes increased participation of Pol δ in the replication of the leading strand.

As mentioned, the Psf1 subunit not only plays a structural role in the CMG complex but is also responsible for contacting Pol ε through the Dpb2 subunit. Thus, the present and previous results indicate that Psf1 or Dpb2 subunit defect, i.e., CMG - Pol ε contact dysfunction results in increased Pol δ contribution to the synthesis on the leading strand. We do not know the exact mechanisms of the increased involvement of Pol δ in the synthesis of the leading strand in the analyzed mutants. In the work describing the effect of *psf1–1* on cell physiology, we proposed possible events leading to the increased participation of Pol δ in leading strand synthesizing [44,50]. Most likely, they also apply to the *dpb2–100* cells.

Since CMG contact with Dpb2 is essential for i/ targeting Pol ε to the leading strand, ii/ stability of Pol ε in the replisome, iii/ proper functioning of Pol ε and CMG, iv/ limitation of the access of Pol δ to this strand and v/ proper positioning of the leading strand template within CMGE, disturbance of any of these mechanisms may result in an increased Pol δ's participation in leading strand replication.

In the previous work, we showed an increase in the frequency of indel mutations in *dpb2* strains, possibly due to polymerase slippage [39]. This indicates instability of Pol ε in the replication fork, which may result in uncoupling from the 3' end, and a more frequent polymerase

switch. In addition, the lack of coordination of CMGE function may give rise to the formation of ssDNA regions that can increase Pol δ recruitment or activate repair processes, i.e. homologous recombination or break-induced replication. It is also possible to assume that in the *dpb2–100* strain, Pol ε, after insertion of an incorrect nucleotide or after encountering DNA damage, may have difficulty binding onto the 3' end of the synthesized strand, allowing Pol δ to access the terminus of the nascent strand.

Mapping of regions in DNA synthesized by Pol δ allowed to propose a model of DNA initiation, according to which on the leading strand, Pol α passes the 3′ end to Pol δ, which, after catching up with the helicase, makes it available for Pol ε [57,71]. In the *dpb2–100* strain, the synthesis by Pol δ after priming may take longer if the cooperation between the helicase and Pol ε is disturbed. In addition, Pol δ can replace Pol ε in situations when the leading strand is unoccupied by a polymerase, such as at the site of replication restart after a stalling event, in the presence of blocking lesions, alternative DNA structures, strand breaks or genomic rearrangements; for review see [76]. Such replacement may occur more frequently when Dpb2 is impaired.

Our earlier studies showed that approximately 50% of the *dpb2–100* mutator effect is due to the increased participation of the error-prone Pol ζ [39,40]. However, it remains an open question what is the source of the remaining mutations. In our earlier work [39], we suggested that increased participation of Pol δ in DNA synthesis in *dpb2–100* strains may be responsible for this mutator effect. The results of the present study also argue for this hypothesis. It is challenging to compare the fidelity of replication of Pol ε and Pol δ because, during replication, they interact to varying degrees and with different components of the replisome, but many data indicate that the error rate of Pol δ is higher than that of Pol ε [77–82]. In addition, if repair processes, i.e., homologous recombination or BIR, are enhanced in the *dpb2–100* cells due to CMGE disintegration and impairment, they may be a significant source of mutagenesis. It has been shown that during HR or BIR, DNA synthesis carried out by Pol δ, especially during synthesis of a sequence with repeated tracts or a sequence that forms alternative structures, can be a significant source of mutations; for review see [76]. Additionally, altered stoichiometry of the Pol ε subunits in the mutant Pol $\varepsilon_{Dpb2-100}$ [39] and the resulting reduced number of the correct Pol ε holoenzymes may favor Pol δ participation in replication of leading strands. Interestingly, it has been shown that reduced levels of Pol ε increase the rates of mitotic recombination, aneuploidy, and single-base mutations [83–85].

Given the previous results with the *psf1–1* allele and the present results with the *dpb2–100* allele, it can be concluded that defects in the non-catalytic subunits of the CMGE complex, such as the Psf1 subunit of the GINS complex or the Dpb2 subunit of the Pol ε complex, may affect the division of labor between the two main replicases. Such defects can affect genome stability and, consequently, the mechanisms of evolution or cause abnormalities in cell physiology. For example, the human FILS syndrome has been described, where a mutation in *POLE1* (encoding the catalytic subunit of Pol ε) was identified that caused alternative splicing that strongly reduced the expression of the *POLE1* and, to a lesser extent, the *POLE2*, encoding the homologue of the yeast Dpb2 subunit. As a consequence, facial dysmorphism, immunodeficiency, livedo, and short stature were observed. Additionally, impaired proliferation and G1- to S-phase progression were observed in T lymphocytes, B lymphocytes, chondrocytes, and osteoblasts from patients [86]. The other case is a patient with combined immunodeficiency, facial dysmorphia, and autoimmunity, with a novel mutation in the gene encoding the DNA polymerase ε subunit 2 (POLE2) [87]. Moreover, *POLE2* was found to be highly expressed in GBM - Glioblastoma - a brain cancer with high morbidity and mortality worldwide [88]. Also, in the IMAGe syndrome [89], patients with reduced Pol ε levels were identified. There is also a long list of disorders in which polymorphisms or overexpression of genes encoding replisome components have been detected; for review see [36,37]. These results underscore the need to study the physiological consequences associated with defects in not only catalytic but also non-catalytic components of the replisome.

4. Materials and methods

4.1. Yeast strains

A list of *S. cerevisiae* strains used in this study for the analyses of mutation spectra is shown in Table S6. They are derivatives of YTAK001, YTAK002 [43], SNM12, SNM24 [90], and SNM70, SNM79 [59] strains (Table S6), kindly provided by T. A. Kunkel (NIEHS, USA). These parental strains contained the *URA3* reporter in the *AGP1*. The reporter gene was cloned in two orientations, [OR1] and [OR2], in respect to the nearest origin of replication (ARS306). Additionally, strains SNM12 and SNM24 contained the *pol3-L612M* allele while strains SNM70 and SNM79 contained the *pol2-M644G* allele. To disrupt *REV3* and *MSH6* PCR-amplified DNA cassettes: *rev3*Δ::*NAT1* (using primers Rev3_UPTEF and Rev3_DNTEF and pAG25 [91] as template) and *msh6*Δ::*HPH* (using primers msh6UTEF and msh6DTEF and pAG32 [91] as template), respectively were used (Table S7). Replacement of *REV3* by *NAT1* in nourseothricin-resistant transformants was verified by multiplex PCR with primer sets Rev3-R4 – Rev3A – nat1UO and Rev3-F4 – Rev3D – nat1DO (Table S7). The *DPB2-LEU2* and *dpb2–100-LEU2* alleles were introduced into yeast cells using the *Pst*I-*Hin*dIII DNA fragments from plasmid pLD2 and pLD2–100, respectively (Fig. S1). Replacement of *MSH6* with *HPH* in hygromycin-resistant transformants was verified by multiplex PCR with primers MSH6-UO – msh6up2 – HPH-UO and MSH6-DO – msh6dw2 – HPH-DO (Table S7). The *pol3-L612M rev3*Δ *dpb2–100 msh6*Δ and *pol2-M644G rev3*Δ *dpb2–100 msh6*Δ strains were also obtained by tetrad dissection from heterozygous diploid strains.

4.2. Media and growth conditions

S. cerevisiae cells were grown at 23 or 30 °C in standard media: YPD (1% Bacto-yeast extract, 2% Bacto-peptone, 2% glucose liquid or solidified with 2% Bacto-agar) supplemented when required with hygromycin B 300 μg/ml (Bioshop, Burlington, Canada) or nourseothricin 100 μg/ml (Werner BioAgents, Jena, Germany). SD medium (0.67% yeast nitrogen base without amino acids, 2% glucose, liquid or solidified with 2% Bacto-agar) supplemented with appropriate amino acids and nitrogenous bases were used for nutrition selection. For selection of *URA3* mutants and mutagenesis assays, SD medium supplemented with 1 mg/ml 5-fluoroorotic acid (5-FOA) (US Biological, Salem, MA, USA) was used [92]. Transformation of *S. cerevisiae* was done using the LiAc/ssDNA/PEG method [93]. For the isolation of yeast chromosomal DNA the Genomic Mini AX Yeast Spin Kit (A&A Biotechnology, Gdansk, Poland) was used.

4.3. Analysis of mutation rates and spectra

Mutation rates were calculated for at least 7 cultures of 2–3 independent yeast isolates for each genotype. Yeast cells were cultured in 2 ml of liquid SD medium supplemented with the required amino acids and nitrogenous bases at 23 °C until stationary phase. After dilution, they were plated on nonselective media and media supplemented with 5-FOA for selection of *URA3* mutants. Colonies were counted after 4–7 days-growth at 23 °C. To calculate mutation rates the $\mu = f/ln(N\mu)$ [μ - mutation rate per round of DNA replication; f - mutant frequency (cell count from selective media divided by the cell count from nonselective media), and N - total population] equation was used [94]. Median values, 95% confidence intervals, and statistical significance of differences in the mutation rates between the respective strains (measured using the nonparametric Mann-Whitney U test) were calculated using GraphPad Prism software. The homogeneity of odds ratios was tested using the calculator (https://www.prostatservices.com/blog/calculator-for-breslow-day-and-tarone-tests-for-homogeneity-of-odds-ratios).

To determine the mutation spectrum in the *URA3* reporter gene, 103–172 5-FOA-resistant colonies obtained from independent cultures were analyzed for each strain under study. For *URA3* sequencing, the gene was amplified by PCR with primers URA3F393 and URA3R412 (Table S7). These primers were also used for sequencing of the PCR product. To calculate the proportion each type of mutation in overall mutagenesis, the number of specific events was divided by the total number of mutations found in a given strain. Then, specific mutations rates were calculated according to their contribution to the overall mutagenesis spectrum. Differences in contribution of each substitution to overall mutagenesis in two strains to be compared were analyzed using contingency table and chi-square statistics. The *p* values for differences in mutation spectra were calculated using Fisher's Exact test (GraphPad Prism software).

4.4. FACS analysis of cell cycle progression

For flow cytometry analysis of *DPB2* and *dpb2–100* cells were cultured at 23 °C and after treatment as described previously [27] were stained using 0.5 μM SYTOX Green (Invitrogen, Carlsbad, CA, USA). Then, the fluorescence signal FL1 was measured using Becton Dickinson FACS Calibur and CellQuest software (BD Bioscience, San Jose, CA, United States) and analysed using Flowing Software (http://www.flowingsoftware.com) to determine the DNA content.

4.5. Measurement of dNTP pools

The dNTPs concentrations were determined as previously described [95]. The analysis was performed for six *dpb2–100* strains (SC234) and four control wild-type strains (SC228) at the permissive temperature 23 °C. For statistical analysis of the dNTP balance, contingency table and the chi-square test were used.

Funding

This research is funded by the National Science Centre, Poland [2015/17/B/NZ1/00850] to I.J.F. Work in the A.C. lab is supported by the Swedish Cancer Society and the Swedish Research Council. The funders had no role in study design, collection, analysis, and interpretation of data, writing of the report, or decision to submit the article for publication.

CRediT authorship contribution statement

Michal Dmowski: Conceptualization, Investigation, Validation, Formal analysis, Visualization, Writing – original draft, Writing – review & editin. **Karolina Makiela-Dzbenska:** Investigation. **Sushma Sharma:** Investigation. **Andrei Chabes:** Validation. **Iwona J. Fijalkowska:** Conceptualization, Validation, Funding acquisition, Writing – review & editing.

Declaration of Competing Interest

The authors declare that there are no conflicts of interest.

Data Availability

Data will be made available on request.

Acknowledgements

We are grateful to Malgorzata Jedrychowska, Ewa Szwajczak, Milena Denkiewicz-Kruk, and Alina Krasilia for excellent technical support and to Krystian Lazowski for valuable comments on the manuscript. We thank T. A. Kunkel (NIHES, USA) for providing yeast strains YTAK001, YTAK002, SNM12, SNM24, SNM70 and SNM79.

Appendix A. Supporting information

Supplementary data associated with this article can be found in the online version at doi:10.1016/j.dnarep.2023.103541.

References

[1] T.A. Guilliam, J.T.P. Yeeles, An updated perspective on the polymerase division of labor during eukaryotic DNA replication, Crit. Rev. Biochem Mol. Biol. 55 (2020) 469–481, https://doi.org/10.1080/10409238.2020.1811630.
[2] L. Pellegrini, The pol α-primase complex, Subcell. Biochem. (2012) 157–169, https://doi.org/10.1007/978-94-007-4572-8_9.
[3] K.J. Gerik, K.J. Gerik, A. Pautz, A. Pautz, Characterization of the two small subunits of *Saccharomyces cerevisiae* DNA polymerase δ, Mol. Biol. 273 (1998) 19747–19755, https://doi.org/10.1074/jbc.273.31.19747.
[4] M. Simon, L. Giot, G. Faye, The 3' to 5' exonuclease activity located in the DNA polymerase δ subunit of Saccharomyces cerevisiae is required for accurate replication, EMBO J. 10 (1991) 2165–2170, https://doi.org/10.1002/j.1460-2075.1991.tb07751.x.
[5] O. Chilkova, B.-H. Jonsson, E. Johansson, The quaternary structure of DNA polymerase epsilon from Saccharomyces cerevisiae, J. Biol. Chem. 278 (2003) 14082–14086, https://doi.org/10.1074/jbc.M211818200.
[6] A. Morrison, H. Araki, A.B. Clark, R.K. Hamatake, A. Sugino, A third essential DNA polymerase in S. cerevisiae, Cell 62 (1990) 1143–1151, https://doi.org/10.1016/0092-8674(90)90391-Q.
[7] A. Morrison, J.B. Bell, T.A. Kunkel, A. Sugino, Eukaryotic DNA polymerase amino acid sequence required for 3'——5' exonuclease activity, Proc. Natl. Acad. Sci. USA 88 (1991) 9473–9477, https://doi.org/10.1073/pnas.88.21.9473.
[8] M. Hogg, P. Osterman, G.O. Bylund, R.A. Ganai, E.B. Lundström, A.E. Sauer-Eriksson, et al., Structural basis for processive DNA synthesis by yeast DNA polymerase É, Nat. Struct. Mol. Biol. 21 (2014) 49–55, https://doi.org/10.1038/nsmb.2712.
[9] T.H. Tahirov, K.S. Makarova, I.B. Rogozin, Y.I. Pavlov, E.V. Koonin, Evolution of DNA polymerases: an inactivated polymerase-exonuclease module in Pol ε and a chimeric origin of eukaryotic polymerases from two classes of archaeal ancestors, Biol. Direct 11 (2009) 1–11, https://doi.org/10.1186/1745-6150-4-11.
[10] R. Dua, D.L. Levy, J.L. Campbell, Analysis of the essential functions of the C-terminal protein/protein interaction domain of *Saccharomyces cerevisiae* pol ε and its unexpected ability to support growth in the absence of the DNA polymerase domain, J. Biol. Chem. 274 (1999) 22283–22288, https://doi.org/10.1074/jbc.274.32.22283.
[11] W. Feng, G. D'Urso, Schizosaccharomyces pombe cells lacking the amino-terminal catalytic domains of DNA polymerase epsilon are viable but require the DNA damage checkpoint control, Mol. Cell Biol. 21 (2001) 4495–4504, https://doi.org/10.1128/MCB.21.14.4495.
[12] L.D. Langston, D. Zhang, O. Yurieva, R.E. Georgescu, J. Finkelstein, N.Y. Yao, et al., CMG helicase and DNA polymerase ε form a functional 15-subunit holoenzyme for eukaryotic leading-strand DNA replication, Proc. Natl. Acad. Sci. USA 111 (2014) 15390–15395, https://doi.org/10.1073/pnas.1418334111.
[13] J. Sun, Y. Shi, R.E. Georgescu, Z. Yuan, B.T. Chait, H. Li, et al., The architecture of a eukaryotic replisome, Nat. Struct. Mol. Biol. 22 (2015) 1–9, https://doi.org/10.1038/nsmb.3113.
[14] Y. Takayama, Y. Kamimura, M. Okawa, S. Muramatsu, A. Sugino, H. Araki, GINS, a novel multiprotein complex required for chromosomal DNA replication in budding yeast, Genes Dev. 17 (2003) 1153–1165, https://doi.org/10.1101/gad.1065903.
[15] P. Goswami, F. Abid Ali, M.E. Douglas, J. Locke, A. Purkiss, A. Janska, et al., Structure of DNA-CMG-Pol epsilon elucidates the roles of the non-catalytic polymerase modules in the eukaryotic replisome, Nat. Commun. 9 (2018) 5061, https://doi.org/10.1038/s41467-018-07417-1.
[16] Z. Yuan, R. Georgescu, L. Bai, D. Zhang, H. Li, M.E. O'Donnell, DNA unwinding mechanism of a eukaryotic replicative CMG helicase, Nat. Commun. 11 (2020) 1–10, https://doi.org/10.1038/s41467-020-14577-6.
[17] H. Araki, R.K. Hamatake, L.H. Johnston, A. Sugino, DPB2, the gene encoding DNA polymerase II subunit B, is required for chromosome replication in Saccharomyces cerevisiae, Proc. Natl. Acad. Sci. USA 88 (1991) 4601–4605, https://doi.org/10.1073/pnas.88.11.4601.
[18] L. Aravind, E.V. Koonin, Phosphoesterase domains associated with DNA polymerases of diverse origins, Nucleic Acids Res 26 (1998) 3746–3752, https://doi.org/10.1093/nar/26.16.3746.
[19] E.V. Koonin, Y.I. Wolf, L. Aravind, Protein fold recognition using sequence profiles and its application in structural genomics, Adv. Protein Chem. 54 (2000) 245–275, https://doi.org/10.1016/s0065-3233(00)54008-x.
[20] A.G. Baranovskiy, J. Gu, N.D. Babayeva, I. Kurinov, Y.I. Pavlov, T.H. Tahirov, Crystal structure of the human Polε B-subunit in complex with the C-terminal domain of the catalytic subunit, J. Biol. Chem. 292 (2017) 15717–15730, https://doi.org/10.1074/jbc.M117.792705.
[21] T. Nuutinen, H. Tossavainen, K. Fredriksson, P. Pirilä, P. Permi, H. Pospiech, et al., The solution structure of the amino-terminal domain of human DNA polymerase ε subunit B is homologous to C-domains of AAA+ proteins, Nucleic Acids Res. 36 (2008) 5102–5110, https://doi.org/10.1093/nar/gkn497.
[22] Z. Yuan, R. Georgescu, G.D. Schauer, M.E. O'Donnell, H. Li, Structure of the polymerase ε holoenzyme and atomic model of the leading strand replisome, Nat. Commun. 11 (2020) 1–11, https://doi.org/10.1038/s41467-020-16910-5.

[23] E. Grabowska, U. Wronska, M. Denkiewicz, M. Jaszczur, A. Respondek, M. Alabrudzinska, et al., Proper functioning of the GINS complex is important for the fidelity of DNA replication in yeast, Mol. Microbiol. 92 (2014) 659–680, https://doi.org/10.1111/mmi.12580.
[24] S. Sengupta, F. Van Deursen, G. De Piccoli, K. Labib, Dpb2 integrates the leading-strand DNA polymerase into the eukaryotic replisome, Curr. Biol. 23 (2013) 543–552, https://doi.org/10.1016/j.cub.2013.02.011.
[25] M. Jaszczur, K. Flis, J. Rudzka, J. Kraszewska, M.E. Budd, P. Polaczek, et al., Dpb2p, a noncatalytic subunit of DNA polymerase ε, contributes to the fidelity of DNA replication in *Saccharomyces cerevisiae*, Genetics 178 (2008) 633–647, https://doi.org/10.1534/genetics.107.082818.
[26] M. Jaszczur, J. Rudzka, J. Kraszewska, K. Flis, P. Polaczek, J.L. Campbell, et al., Defective interaction between Pol2p and Dpb2p, subunits of DNA polymerase epsilon, contributes to a mutator phenotype in Saccharomyces cerevisiae, Mutat. Res. 669 (2009) 27–35, https://doi.org/10.1016/j.mrfmmm.2009.04.012.
[27] M. Dmowski, J. Rudzka, J.L. Campbell, P. Jonczyk, I.J. Fijałkowska, Mutations in the non-catalytic subunit Dpb2 of DNA polymerase epsilon affect the Nrm1 branch of the DNA replication checkpoint, PLOS Genet. 13 (2017), e1006572, https://doi.org/10.1371/journal.pgen.1006572.
[28] V.P. Bermudez, A. Farina, V. Raghavan, I. Tappin, J. Hurwitz, Studies on human DNA polymerase epsilon and GINS complex and their role in DNA replication, J. Biol. Chem. 286 (2011) 28963–28977, https://doi.org/10.1074/jbc.M111.256289.
[29] J.T.P. Yeeles, J. Poli, K.J. Marians, P. Pasero, Rescuing stalled or damaged replication forks, Cold Spring Harb. Perspect. Biol. 5 (2013) 1–16, https://doi.org/10.1101/cshperspect.a012815.
[30] K. Hizume, S. Endo, S. Muramatsu, T. Kobayashi, H. Araki, DNA polymerase ε-dependent modulation of the pausing property of the CMG helicase at the barrier, Genes Dev. 32 (2018) 1315–1320, https://doi.org/10.1101/gad.317073.118.
[31] J.C. Zhou, A. Janska, P. Goswami, L. Renault, F. Abid Ali, A. Kotecha, et al., CMG–Pol epsilon dynamics suggests a mechanism for the establishment of leading-strand synthesis in the eukaryotic replisome, Proc. Natl. Acad. Sci. 114 (2017), 201700530, https://doi.org/10.1073/pnas.1700530114.
[32] H. Araki, R.K. Hamatake, A. Morrison, A.L. Johnson, L.H. Johnston, A. Sugino, Cloning DPB3, the gene encoding the third subunit of DNA polymerase II of Saccharomyces cerevisiae, Nucleic Acids Res. 19 (1991) 4867–4872, https://doi.org/10.1093/nar/19.18.4867.
[33] T. Ohya, S. Maki, Y. Kawasaki, A. Sugino, Structure and function of the fourth subunit (Dpb4p) of DNA polymerase epsilon in *Saccharomyces cerevisiae*, Nucleic Acids Res. 28 (2000) 3846–3852 (Available), ⟨http://www.pubmedcentral.nih.gov/articlerender.fcgi?artid=110797&tool=pmcentrez&rendertype=abstract⟩.
[34] T. Iida, H. Araki, Noncompetitive counteractions of DNA polymerase ε and ISW2/yCHRAC for epigenetic inheritance of telomere position effect in saccharomyces cerevisiae, Mol. Cell. Biol. (2004) 217–227, https://doi.org/10.1128/mcb.24.1.217-227.2004.
[35] A.J. Tackett, D.J. Dilworth, M.J. Davey, M. O'Donnell, J.D. Aitchison, M.P. Rout, et al., Proteomic and genomic characterization of chromatin complexes at a boundary, J. Cell Biol. 169 (2005) 35–47, https://doi.org/10.1083/jcb.200502104.
[36] M. Schmit, A.K. Bielinsky, Congenital diseases of DNA replication: clinical phenotypes and molecular mechanisms, Int J. Mol. Sci. 22 (2021) 1–38, https://doi.org/10.3390/ijms22020911.
[37] R. Bellelli, S.J. Boulton, Spotlight on the replisome: aetiology of DNA replication-associated genetic diseases, Trends Genet 37 (2021) 317–336, https://doi.org/10.1016/j.tig.2020.09.008.
[38] J. Cottineau, M.C. Kottemann, F.P. Lach, Y.H. Kang, F. Vély, E.K. Deenick, et al., Inherited GINS1 deficiency underlies growth retardation along with neutropenia and NK cell deficiency, J. Clin. Invest 127 (2017) 1991–2006, https://doi.org/10.1172/JCI90727.
[39] M. Garbacz, H. Araki, K. Flis, A. Bebenek, A.E. Zawada, P. Jonczyk, et al., Fidelity consequences of the impaired interaction between DNA polymerase epsilon and the GINS complex, DNA Repair (Amst.) 29 (2015) 23–35, https://doi.org/10.1016/j.dnarep.2015.02.007.
[40] J. Kraszewska, M. Garbacz, P. Jonczyk, I.J. Fijalkowska, M. Jaszczur, Defect of Dpb2p, a noncatalytic subunit of DNA polymerase ε, promotes error prone replication of undamaged chromosomal DNA in *Saccharomyces cerevisiae*, Mutat. Res. 737 (2012) 34–42, https://doi.org/10.1016/j.mrfmmm.2012.06.002.
[41] A.A. Larrea, S.A. Lujan, S.A. Nick McElhinny, P.A. Mieczkowski, M.A. Resnick, D. A. Gordenin, et al., Genome-wide model for the normal eukaryotic DNA replication fork, Proc. Natl. Acad. Sci. USA 107 (2010) 17674–17679, https://doi.org/10.1073/pnas.1010178107.
[42] S.A. Nick McElhinny, D.A. Gordenin, C.M. Stith, P.M.J. Burgers, T.A. Kunkel, Division of labor at the eukaryotic replication fork, Mol. Cell 30 (2008) 137–144, https://doi.org/10.1016/j.molcel.2008.02.022.
[43] Z.F. Pursell, I. Isoz, E.-B. Lundström, E. Johansson, T.A. Kunkel, Yeast DNA polymerase ε participates in leading-strand DNA replication, Science 317 (2007) 127–130, https://doi.org/10.1126/science.1144067.
[44] M. Dmowski, M. Jedrychowska, K. Makiela-Dzbenska, M. Denkiewicz-kruk, S. Sharma, A. Chabes, et al., Increased contribution of DNA polymerase delta to the leading strand replication in yeast with an impaired CMG helicase complex, DNA Repair (Amst.) 110 (2022), 103272, https://doi.org/10.1016/j.dnarep.2022.103272.
[45] S.A. Nick McElhinny, C.M. Stith, P.M.J. Burgers, T.A. Kunkel, Inefficient proofreading and biased error rates during inaccurate DNA synthesis by a mutant derivative of *Saccharomyces cerevisiae* DNA polymerase, J. Biol. Chem. 282 (2007) 2324–2332, https://doi.org/10.1074/jbc.M609591200.
[46] M.A. Garbacz, P.B. Cox, S. Sharma, S.A. Lujan, A. Chabes, T.A. Kunkel, The absence of the catalytic domains of Saccharomyces cerevisiae DNA polymerase strongly reduces DNA replication fidelity, Nucleic Acids Res. 47 (2019) 3986–3995, https://doi.org/10.1093/nar/gkz048.
[47] S.A. Lujan, A.R. Clausen, A.B. Clark, H.K. MacAlpine, D.M. MacAlpine, E.P. Malc, et al., Heterogeneous polymerase fidelity and mismatch repair bias genome variation and composition, Genome Res. 24 (2014) 1751–1764, https://doi.org/10.1101/gr.178335.114.
[48] R.E. Johnson, R. Klassen, L. Prakash, S. Prakash, A major role of DNA polymerase δ in replication of both the leading and lagging DNA strands, Mol. Cell 59 (2015) 163–175, https://doi.org/10.1016/j.molcel.2015.05.038.
[49] M. Miyazawa-Onami, H. Araki, S. Tanaka, Pre-initiation complex assembly functions as a molecular switch that splits the Mcm2–7 double hexamer, EMBO Rep. 18 (2017) 1752–1761, https://doi.org/10.15252/embr.201744206.
[50] M. Dmowski, K. Makiela-Dzbenska, M. Jedrychowska, M. Denkiewicz-Kruk, I. J. Fijalkowska, Mutation spectrum data for Saccharomyces cerevisiae psf1-1 pol2-M644G mutants, Data Br. 42 (2022), 108223, https://doi.org/10.1016/j.dib.2022.108223.
[51] Y.I. Pavlov, C. Frahm, S.A.N. McElhinny, A. Niimi, M. Suzuki, T.A. Kunkel, Evidence that errors made by DNA polymerase α are corrected by DNA polymerase δ, Curr. Biol. 16 (2006) 202–207, https://doi.org/10.1016/j.cub.2005.12.002.
[52] I. Miyabe, T. a Kunkel, A.M. Carr, The major roles of DNA polymerases epsilon and delta at the eukaryotic replication fork are evolutionarily conserved, PLoS Genet. 7 (2011), e1002407, https://doi.org/10.1371/journal.pgen.1002407.
[53] Y. Daigaku, A. Keszthelyi, C.A. Müller, I. Miyabe, T. Brooks, R. Retkute, et al., A global profile of replicative polymerase usage, Nat. Struct. Mol. Biol. 22 (2015) 192–198, https://doi.org/10.1038/nsmb.2962.
[54] S.A. Lujan, J.S. Williams, Z.F. Pursell, A.A. Abdulovic-Cui, A.B. Clark, S.A. Nick McElhinny, et al., Mismatch repair balances leading and lagging strand DNA replication fidelity, PLoS Genet. 8 (2012), https://doi.org/10.1371/journal.pgen.1003016.
[55] S.A. Lujan, J.S. Williams, T.A. Kunkel, DNA polymerases divide the labor of genome replication, Trends Cell Biol. 26 (2016) 1–15, https://doi.org/10.1016/j.tcb.2016.04.012.
[56] A.R. Clausen, S.A. Lujan, A.B. Burkholder, C.D. Orebaugh, J.S. Williams, M. F. Clausen, et al., Tracking replication enzymology in vivo by genome-wide mapping of ribonucleotide incorporation, Nat. Struct. Mol. Biol. 22 (2015) 185–191, https://doi.org/10.1038/nsmb.2957.
[57] Z.X. Zhou, S.A. Lujan, A.B. Burkholder, M.A. Garbacz, T.A. Kunkel, Roles for DNA polymerase δ in initiating and terminating leading strand DNA replication, Nat. Commun. 10 (2019) 1–10, https://doi.org/10.1038/s41467-019-11995-z.
[58] M.A.M. Reijns, H. Kemp, J. Ding, S.M. De Procé, A.P. Jackson, M.S. Taylor, Lagging-strand replication shapes the mutational landscape of the genome, Nature 518 (2015) 502–506, https://doi.org/10.1038/nature14183.
[59] S.A. Nick McElhinny, D. Kumar, A.B. Clark, D.L. Watt, E. Brian, E. Lundström, et al., Genome instability due to ribonucleotide incorporation into DNA, Nat. Chem. Biol. 6 (2010) 774–781, https://doi.org/10.1038/nchembio.424.
[60] O. Chilkova, P. Stenlund, I. Isoz, C.M. Stith, P. Grabowski, E.-B. Lundström, et al., The eukaryotic leading and lagging strand DNA polymerases are loaded onto primer-ends via separate mechanisms but have comparable processivity in the presence of PCNA, Nucleic Acids Res 35 (2007) 6588–6597, https://doi.org/10.1093/nar/gkm741.
[61] J.T.P. Yeeles, T.D. Deegan, A. Janska, A. Early, J.F.X. Diffley, Regulated eukaryotic DNA replication origin firing with purified proteins, Nature 519 (2015) 431–435, https://doi.org/10.1038/nature14285.
[62] R.E. Georgescu, L. Langston, N.Y. Yao, O. Yurieva, D. Zhang, J. Finkelstein, et al., Mechanism of asymmetric polymerase assembly at the eukaryotic replication fork, Nat. Struct. Mol. Biol. 21 (2014) 664–670, https://doi.org/10.1038/nsmb.2851.
[63] R.E. Georgescu, G.D. Schauer, N.Y. Yao, L.D. Langston, O. Yurieva, D. Zhang, et al., Reconstitution of a eukaryotic replisome reveals suppression mechanisms that define leading/lagging strand operation, Elife 4 (2015), e04988, https://doi.org/10.7554/eLife.04988.
[64] L. Bai, Z. Yuan, J. Sun, R. Georgescu, M.E. O'Donnell, H. Li, in: H. Masai, M. Foiani (Eds.), Architecture of the Saccharomyces cerevisiae Replisome BT - DNA Replication: From Old Principles to New Discoveries, Springer Singapore, Singapore, 2017, pp. 207–228, https://doi.org/10.1007/978-981-10-6955-0_10.
[65] Y.V. Fu, H. Yardimci, D.T. Long, T.V. Ho, A. Guainazzi, V.P. Bermudez, et al., Selective bypass of a lagging strand roadblock by the eukaryotic replicative DNA helicase, Cell 7 (2011) 931–941, https://doi.org/10.1016/j.cell.2011.07.045.
[66] R. Georgescu, Z. Yuan, L. Bai, R. de Luna Almeida Santos, J. Sun, D. Zhang, et al., Structure of eukaryotic CMG helicase at a replication fork and implications to replisome architecture and origin initiation, Proc. Natl. Acad. Sci. (2017), 201620500, https://doi.org/10.1073/pnas.1620500114.
[67] E. Johansson, P. Garg, P.M.J. Burgers, The Pol32 subunit of DNA polymerase δ contains separable domains for processive replication and proliferating cell nuclear antigen (PCNA) binding, J. Biol. Chem. 279 (2004) 1907–1915, https://doi.org/10.1074/JBC.M310362200.
[68] J.T.P. Yeeles, A. Janska, A. Early, J.F.X. Diffley, How the eukaryotic replisome achieves rapid and efficient DNA replication, Mol. Cell 65 (2017) 105–116, https://doi.org/10.1016/j.molcel.2016.11.017.
[69] R.A. Donnianni, Z.X. Zhou, S.A. Lujan, A. Al-Zain, V. Garcia, E. Glancy, et al., DNA polymerase delta synthesizes both strands during break-induced replication, Mol. Cell 76 (2019) 371–381.e4, https://doi.org/10.1016/j.molcel.2019.07.033.
[70] V. Aria, J.T.P. Yeeles, Mechanism of bidirectional leading-strand synthesis establishment at eukaryotic DNA replication origins, Mol. Cell 73 (2019) 199–211.e10, https://doi.org/10.1016/j.molcel.2018.10.019.

[71] M.A. Garbacz, S.A. Lujan, A.B. Burkholder, P.B. Cox, Q. Wu, Z.X. Zhou, et al., Evidence that DNA polymerase δ contributes to initiating leading strand DNA replication in *Saccharomyces cerevisiae*, Nat. Commun. 9 (2018) 1–11, https://doi.org/10.1038/s41467-018-03270-4.
[72] I. Miyabe, K. Mizuno, A. Keszthelyi, Y. Daigaku, M. Skouteri, S. Mohebi, et al., Polymerase δ replicates both strands after homologous recombination–dependent fork restart, Nat. Struct. Mol. Biol. (2015) 1–8, https://doi.org/10.1038/nsmb.3100.
[73] C.R. Bulock, X. Xing, P.V. Shcherbakova, DNA polymerase δ proofreads errors made by DNA polymerase ε, Proc. Natl. Acad. Sci. USA 117 (2020) 6035–6041, https://doi.org/10.1073/pnas.1917624117.
[74] C.L. Flood, G.P. Rodriguez, G. Bao, A.H. Shockley, Y.W. Kow, G.F. Crouse, Replicative DNA polymerase δ but not ε proofreads errors in cis and in trans, PLOS Genet. 11 (2015), e1005049, https://doi.org/10.1371/journal.pgen.1005049.
[75] A. Aksenova, K. Volkov, J. Maceluch, Z.F. Pursell, I.B. Rogozin, T. a Kunkel, et al., Mismatch repair-independent increase in spontaneous mutagenesis in yeast lacking non-essential subunits of DNA polymerase ε, PLoS Genet. 6 (2010), e1001209 https://doi.org/10.1371/journal.pgen.1001209.
[76] M.J. Prindle, L.A. Loeb, DNA polymerase delta in dna replication and genome maintenance, Environ. Mol. Mutagen 53 (2012) 666–682, https://doi.org/10.1002/em.21745.
[77] K. Shimizu, K. Hashimoto, J.M. Kirchner, W. Nakai, H. Nishikawa, M.A. Resnick, et al., Fidelity of DNA polymerase ε holoenzyme from budding yeast Saccharomyces cerevisiae, J. Biol. Chem. 277 (2002) 37422–37429, https://doi.org/10.1074/jbc.M204476200.
[78] K. Hashimoto, K. Shimizu, N. Nakashima, A. Sugino, Fidelity of DNA polymerase δ holoenzyme from saccharomyces cerevisiae: the sliding clamp proliferating cell nuclear antigen decreases its fidelity, Vitro 42 (2003) 14207–14213, https://doi.org/10.1021/bi0348359.
[79] J.M. Fortune, Y.I. Pavlov, C.M. Welch, E. Johansson, P.M.J. Burgers, T.A. Kunkel, Saccharomyces cerevisiae DNA Polymerase δ: High fidelity for base substitutions but lower fidelity for single-and multi-base deletions, J. Biol. Chem. 280 (2005) 29980–29987, https://doi.org/10.1074/jbc.M505236200.
[80] P.V. Shcherbakova, Y.I. Pavlov, O. Chilkova, I.B. Rogozin, E. Johansson, T. A. Kunkel, Unique error signature of the four-subunit yeast DNA polymerase ε, J. Biol. Chem. 278 (2003) 43770–43780, https://doi.org/10.1074/jbc.M306893200.
[81] L.M. Dieckman, R.E. Johnson, S. Prakash, M.T. Washington, Pre-steady state kinetic studies of the fidelity of nucleotide incorporation by yeast DNA polymerase ?? Biochemistry 49 (2010) 7344–7350, https://doi.org/10.1021/bi100556m.
[82] K.A. Johnson, The kinetic and chemical mechanism of high-fidelity DNA polymerases, Biochim Biophys. Acta - Proteins Proteom. 1804 (2010) 1041–1048, https://doi.org/10.1016/j.bbapap.2010.01.006.
[83] K. Zhang, Y. Sui, W.L. Li, G. Chen, X.C. Wu, R.J. Kokoska, et al., Global genomic instability caused by reduced expression of DNA polymerase ε in yeast, Proc. Natl. Acad. Sci. USA (2022), https://doi.org/10.1073/pnas.2119588119.
[84] D.-Q. Zheng, T. Petes, D.-Q. Zheng, T.D. Petes, Genome instability induced by low levels of replicative DNA polymerases in yeast, Genes (Basel) 9 (2018) 539, https://doi.org/10.3390/genes9110539.
[85] Y. Sui, L. Qi, K. Zhang, N. Saini, L.J. Klimczak, C.J. Sakofsky, et al., Analysis of APOBEC-induced mutations in yeast strains with low levels of replicative DNA polymerases, Proc. Natl. Acad. Sci. USA 117 (2020) 9440–9450, https://doi.org/10.1073/pnas.1922472117.
[86] J. Pachlopnik Schmid, R. Lemoine, N. Nehme, V. Cormier-Daire, P. Revy, F. Debeurme, et al., Polymerase ε1 mutation in a human syndrome with facial dysmorphism, immunodeficiency, livedo, and short stature ("FILS syndrome"), J. Exp. Med 209 (2012) 2323–2330, https://doi.org/10.1084/jem.20121303.
[87] F. Frugoni, K. Dobbs, K. Felgentreff, H. Aldhekri, B.K. Al Saud, R. Arnaout, et al., A novel mutation in the POLE2 gene causing combined immunodeficiency, J. Allergy Clin. Immunol. 137 (2016) 635–638.e1, https://doi.org/10.1016/j.jaci.2015.06.049.
[88] P. Zhang, X. Chen, L.Y. Zhang, D. Cao, Y. Chen, Z.Q. Guo, et al., POLE2 facilitates the malignant phenotypes of glioblastoma through promoting AURKA-mediated stabilization of FOXM1, Cell Death Dis. 13 (2022) 1–10, https://doi.org/10.1038/s41419-021-04498-7.
[89] C.V. Logan, J.E. Murray, D.A. Parry, A. Robertson, R. Bellelli, Ž. Tarnauskaitė, et al., DNA polymerase epsilon deficiency causes IMAGe syndrome with variable immunodeficiency, Am. J. Hum. Genet 103 (2018) 1038–1044, https://doi.org/10.1016/j.ajhg.2018.10.024.
[90] S.A. Nick McElhinny, G.E. Kissling, T.A. Kunkel, Differential correction of lagging-strand replication errors made by DNA polymerases α and δ, Proc. Natl. Acad. Sci. USA 107 (2010) 21070–21075, https://doi.org/10.1073/pnas.1013048107.
[91] A.L. Goldstein, J.H. McCusker, Three new dominant drug resistance cassettes for gene disruption in Saccharomyces cerevisiae, Yeast 15 (1999) 1541–1553, https://doi.org/10.1002/(SICI)1097-0061(199910)15:14<1541::AID-YEA476>3.0.CO;2-K.
[92] J.D. Boeke, F. LaCroute, G.R. Fink, A positive selection for mutants lacking 5' phosphate decarboxylase activity in yeast: 5 fluoro-orotic acid resistance, Mol. Gen. Genet 197 (1984) 345–346.
[93] R.D. Gietz, R.A. Woods, Transformation of yeast by the lithium acetate/single-stranded carrier DNA/PEG method. Methods in Microbiology, Elsevier,, 1998, https://doi.org/10.1016/S0580-9517(08)70325-8.
[94] J.W. Drake, A constant rate of spontaneous mutation in DNA-based microbes, Proc. Natl. Acad. Sci. 88 (1991) 7160–7164, https://doi.org/10.1073/pnas.88.16.7160.
[95] D.L. Watt, R.J. Buckland, S.A. Lujan, T.A. Kunkel, A. Chabes, Genome-wide analysis of the specificity and mechanisms of replication infidelity driven by imbalanced dNTP pools, Nucleic Acids Res 44 (2015) 1669–1680, https://doi.org/10.1093/nar/gkv1298.